High concentration measurements of U and Pu with non- destructive and standard less K-edge densitometer device

E. Esbelin, C. Rivier, G. Duhamel

High concentration measurements of U and Pu with non-destructive and standard less K-edge densitometer device

E. Esbelin[(1)*], C. Rivier[(1)], G. Duhamel[(2)]

(1) CEA, Nuclear Energy Division, Research Department on Mining and Fuel Recycling Processes, Atalante Analysis Laboratory, BP 17171, 30207 Bagnols sur Cèze, France

** Corresponding author: eric.esbelin@cea.fr*

(2) IAEA, International Atomic Energy Agency, Safeguards Analytical Services, Tokyo Regional Office, Seibunkan Bldg. 9F, 1-5-9 Iidabashi, Tokyo 102-0072, Japan

Abstract

The K-edge densitometry, also called absorption measurement, is based on Beer-Lambert's law to relate the X-ray beam attenuation to the composition properties of the material to be studied. This technique is dedicated to the measurement of high concentrations of U and/or Pu typically above 50 g/L. Its relatively fast analysis time and its high accuracy make it a valuable choice in nuclear fuel reprocessing facilities. This paper presents the results obtained from assay sample with high U and Pu concentrations. Two processing methods without calibration (except energy calibration) are compared and discussed. Despite literature which does not recommend the use of estimated mass attenuation coefficients near edge energy, this study shows that some very good results are obtained with these values for uranium and plutonium concentration estimations, with a bias less than 1%.

Keywords: K-edge densitometer, Uranium, Plutonium, standardless

1 Introduction

The analysis laboratory in the French Alternative Energies and Atomic Energy Commission (CEA) Atalante facility in Marcoule performs analyses for numerous R&D studies carried out in glove-boxes or in hot cells (high activity). Among the analytical devices used, a hybrid K-edge densitometer was designed and set up for the measurements of U and Pu concentrations in high activity solutions. This device is located in the back zone of the analysis shielded line and the sample is transferred by a pneumatic line between the hot cell and the device. Typically, sample of irradiated spent fuel dissolution solutions can be measured without any prior preparation.

The K-edge densitometry can be also called absorption measurement. Beer-Lambert's law is used to relate the X-ray beam attenuation to the composition properties of the material. This system is dedicated to the measurement of high concentrations of U and/or Pu typically above 50 g/L. Its relatively fast analysis time and its high accuracy make it a valuable choice in nuclear fuel reprocessing facilities.

This device has a second measuring channel that corresponds to an energy dispersive X-ray fluorescence (ED-XRF) measurement. Its use is mainly dedicated to the measurement of lower concentrations of U and Pu. The use of absorption channel with fluorescence channel is the cause of the term "hybrid" in the name of this specific device. In the hybrid mode, the absorption result of the first element is used as an internal standard for the data processing of the corresponding XRF spectrum and determination of the second element concentration.

CEA developed its software to process HKED data. Unlike few papers focusing on HKED, this paper presents the results obtained from assay sample with high U and Pu concentrations.

The discussion is therefore only about the data processing of spectra obtained through the absorption channel. Two processing methods without calibration (except energy calibration) are compared and discussed. In order to study the reliability of the algorithm used, some spectra from measured sample solutions of a reprocessing plant were supplied by IAEA. Only acquisition parameters were rent but the reference values were kept unknown by IAEA and were supplied only after the comparison.

2 HKED Device at Atalante

The X-ray generator and X-ray tube (W anode, MG165) are marketed by YXLON. The tube configuration used in the laboratory is 150 kV and 10 mA for assay sample measurement or 5 mA for reference sample measurement. Reference solution, also called blank solution, has the same matrix as the assay sample without U and Pu. The two detectors are hyper-pure Ge crystals (Canberra EGX 200-10, active area 200 mm^2) cooled with liquid nitrogen. The acquisition electronics are Canberra DSA-1000 coupled with Genie 2000 software. The sample is transferred pneumatically from a shielded cell to analytical equipment. The device, located behind the shielded line, is also fully shielded (Pb protection). Figure 1 schematically illustrates the device.

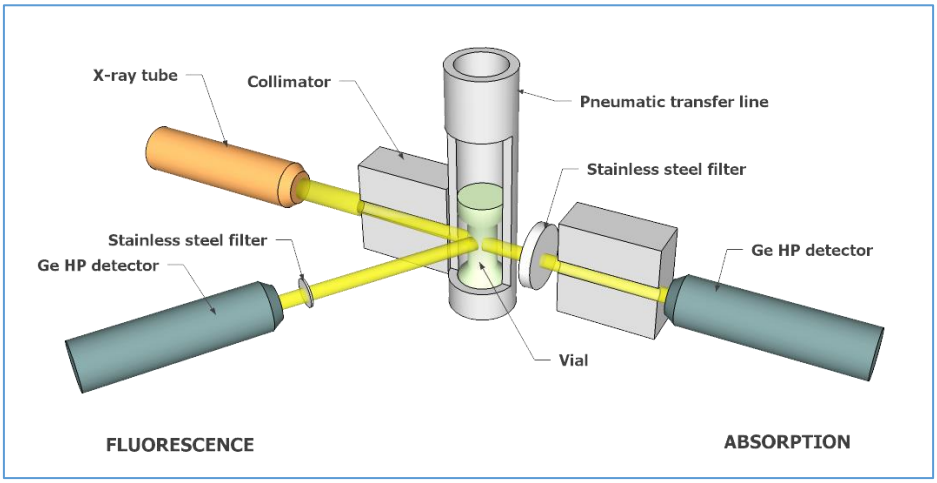

Figure 1. Simplified diagram of the nuclearized high activity HKED. Collimator is not represented on fluorescence path.

The samples are packaged in small polypropylene vials 1.53 cm in diameter and 1.5 mm thick. The primary beam reaches the sample vial laterally after passing through the stainless steel pneumatic transfer tube (1 mm thick).

Stainless steel filters are located between the sample and the detector on each channel. The filter thickness of the fluorescence channel is 1 mm and 10 mm for the absorption channel. The aim of these filters is to decrease the counting rate of lower energies.

Typical counting time is 1000 s and only liquid samples are measured.

Other K-edge densitometers were described in details, for example in [1]. The main difference is the existence of two sample containers: a glass cuvette for absorption measurement and a polyethylene vial for XRF measurement. The use of a glass cuvette gives a better accuracy on path length compared to polyethylene vial.

3 Theory

The attenuation of photons on homogeneous matter is described by the exponential law (Beer Lambert's law):

$$I = I_0 e^{-\mu x} \quad (1)$$

Where I is the transmitted intensity, I_0 is the incident intensity, μ is the mass attenuation coefficient and x is the absorber thickness in centimeters.

If the absorber is a chemical compound or a mixture, its mass attenuation coefficient can be approximately evaluated from the coefficients μ_i of the constituent elements according to the weighted mean:

$$\mu = \sum_{i=1}^{n} W_i \mu_i \quad (2)$$

where W_i is the weight fraction of the *i*th element and n is the total number of the elements in the absorber. It is to notice [2] that this mixture rule ignores changes in the atomic wave function resulting from changes in the molecular, chemical, or crystalline environment of an atom. Above 10 keV, errors from this approximation are expected to be less than a few percent, except in the regions just above absorption edges.

Unlike Collins [3], the mass attenuation coefficient given in this paper is the total mass attenuation coefficient (photoelectric + Compton scattering + Rayleigh scattering).

From equation (1), the transmittance can be defined by:

$$T = \frac{I}{I_0} \quad (1)$$

To simplify the presentation, we distinguish actinides from the other elements of the solution, then for an assay sample with N actinides, the transmittance at energy E can be written as:

$$T_1(E) = \frac{I(E)}{I_0(E)} = e^{-\left(\sum_{i=1}^{N} W_i \mu_i(E) x + \sigma_1(E) x\right)} \quad (4)$$

Where $\sigma_1(E)$ represents the total mass attenuation coefficient of the matrix at energy E.

For a reference sample, called also blank sample, with no actinide, the transmittance at energy E can be written:

$$T_2(E) = \frac{I(E)}{I_0(E)} = e^{-\sigma_2(E) x} \quad (5)$$

3.1 Net intensity

Net intensity is obtained after subtraction of inelastic scattering and pile-up effect occurring in the detector. The method proposed by Ottmar and Eberle [1] has been used:

$$I_C(i) = I_L + (I_R - I_L) \frac{\sum_{j=L}^{j=i} I(j)}{\sum_{j=L}^{j=R} I(j)} \quad (6)$$

Where

$I_C(i)$: background intensity at channel i

$I(j)$: raw intensity at channel j

I_L : mean intensity on left background window

I_R : mean intensity on right background window

Net intensity, only calculated between L and R windows, is obtained by:

$$I^{net}(i) = I(i) - I_C(i) \tag{7}$$

This method is approximate and, to be as rigorous as possible, all the processes of scattering and electronics effects should be taken into account: detector response, step background, escape peak, tailing, shaping, etc. McElroy [4] highlights the various contributors to the KED response while doing a spectral fitting approach.

3.2 General densitometry equations

In order to process spectra obtained with different experimental parameters, mainly current intensity and live time, each net spectrum intensity is normalized to current intensity and live time, then:

$$I = \frac{I^{net}(cps)}{i(mA)\cdot t(s)} \tag{8}$$

Where

i : current intensity of the X-ray tube (mA)

t : live time acquisition(s)

General densitometry equation is defined from the ratio of the assay sample transmittance to the reference sample transmittance:

$$\Gamma(E) = \frac{T_1(E)}{T_2(E)} = \frac{e^{-\left(\sum_{i=1}^{N} W_i \mu_i(E) x + \sigma_1(E) x\right)}}{e^{-\sigma_2(E) x}} = e^{-\left(\sum_{i=1}^{N} W_i \mu_i(E) + \sigma_1(E) - \sigma_2(E)\right) x} \tag{9}$$

Notice that equation (9) is correct only because we assume that the X-ray beam rate is strictly proportional to current intensity, as:

$$\frac{{I_0}^{assay\ sample}}{i^{assay\ sample}.t^{assay\ sample}} = \frac{{I_0}^{reference\ sample}}{i^{reference\ sample}.t^{reference\ sample}} \tag{10}$$

From equation (9), for two energies E_1 and E_2:

$$\frac{\Gamma(E_1)}{\Gamma(E_2)} = e^{-\left(\sum_{i=1}^{N} W_i \Delta\mu_i{}_{E_2}^{E_1} + \Delta\sigma_1{}_{E_2}^{E_1} - \Delta\sigma_2{}_{E_2}^{E_1}\right) x} \tag{11}$$

Where $\Delta\mu_i{}_{E_2}^{E_1} = \mu_i(E_1) - \mu_i(E_2)$ and $\Delta\sigma_j{}_{E_2}^{E_1} = \sigma_j(E_1) - \sigma_j(E_2)$

From equation (11):

$$\sum_i^N \Delta\mu_i{}_{E_2}^{E_1} W_i = \frac{1}{x}\{e^{A_{E_2}} - e^{A_{E_1}}\} - \Delta\sigma_1{}_{E_2}^{E_1} + \Delta\sigma_2{}_{E_2}^{E_1} \tag{12}$$

Where $A_E = ln\left\{ln\frac{1}{\Gamma(E)}\right\}$

3.3 Study cases

For each actinide *j*, a couple of energy, noted (E_j^-,E_j^+), is chosen on both sides to its absorption edge energy E_j.

- **Case 1**: Reference sample and assay sample have the same matrix and for each actinide, energies E_j^- and E_j^+ are chosen very close to absorption edge energy E_j

In this case, $\Delta\sigma_{1\,E_j^-}^{E_j^+} - \Delta\sigma_{2\,E_j^-}^{E_j^+} = 0$ (same matrix) and only $\Delta\mu_{j\,E_j^-}^{E_j^+} \neq 0$ because other actinides have no discontinuity for energy E_j.

The densitometry equation for each actinide j is:

$$\Delta\mu_j(\mathrm{E}_j)W_j = \frac{1}{x}\left\{\mathrm{e}^{A_{E_j^-}} - \mathrm{e}^{A_{E_j^+}}\right\} = \frac{H_j}{x} \qquad (13)$$

- **Case 2**: Reference sample and assay sample have different matrices and for each actinide, energies E_j^- and E_j^+ are chosen very close to absorption edge energy E_j

In this case, $\Delta\sigma_{1\,E_j^-}^{E_j^+} \cong 0$, $\Delta\sigma_{2\,E_j^-}^{E_j^+} \cong 0$ and only $\Delta\mu_{j\,E_j^+}^{E_j^+} \neq 0$ because all other actinides have no discontinuity for the energy E_j.

The good approximation of densitometry equation is equation (13) again.

- **Case 3**: Reference sample and assay sample have the same matrix and for each actinide, energies E_j^- and E_j^+ are not too close to E_j.

In this case, $\Delta\sigma_{1\,E_j^-}^{E_j^+} - \Delta\sigma_{2\,E_j^-}^{E_j^+} = 0$ (same matrix) but $\Delta\mu_{k\,E_j^+}^{E_j^+} \neq 0$ for all the actinides in solution (k in [1..N]).

Thus, the densitometry matrix system to solve for N actinides in solution is:

$$\begin{bmatrix} \Delta\mu_{1\,E_1^-}^{E_1^+} & \cdots & \Delta\mu_{N\,E_1^-}^{E_1^+} \\ \vdots & \ddots & \vdots \\ \Delta\mu_{1\,E_N^-}^{E_N^+} & \cdots & \Delta\mu_{N\,E_N^-}^{E_N^+} \end{bmatrix} \begin{bmatrix} W_1 \\ \vdots \\ W_N \end{bmatrix} = \begin{bmatrix} \mathrm{H}_1 \\ \vdots \\ \mathrm{H}_N \end{bmatrix} \quad \text{with} \quad \mathrm{H}_j = \frac{1}{x}\left\{\mathrm{e}^{A_{j^+}} - \mathrm{e}^{A_{j^-}}\right\} \qquad (14)$$

- **Case 4**: Reference sample and assay sample have different matrices and for each actinide, energies E_j^- and E_j^+ are not too close to E_j.

Unlike the previous case, $\Delta\sigma_{1\,E_j^-}^{E_j^+} - \Delta\sigma_{2\,E_j^-}^{E_j^+} \neq 0$. Thus equation (14) becomes:

$$\begin{bmatrix} \Delta\mu_{1\,E_1^-}^{E_1^+} & \cdots & \Delta\mu_{N\,E_1^-}^{E_1^+} \\ \vdots & \ddots & \vdots \\ \Delta\mu_{1\,E_N^-}^{E_N^+} & \cdots & \Delta\mu_{N\,E_N^-}^{E_N^+} \end{bmatrix} \begin{bmatrix} W_1 \\ \vdots \\ W_N \end{bmatrix} = \begin{bmatrix} \mathrm{H}_1 - \Delta\sigma_{1\,E_1^-}^{E_1^+} + \Delta\sigma_{2\,E_1^-}^{E_1^+} \\ \vdots \\ \mathrm{H}_N - \Delta\sigma_{1\,E_N^-}^{E_N^+} + \Delta\sigma_{2\,E_N^-}^{E_N^+} \end{bmatrix} \qquad (15)$$

4 Data Processing

As underlined in [1], within limited energy ranges the mass attenuation coefficient of an actinide i can be represented by a power function:

$$\mu_i(E) = a_i E^{-b_i} \qquad (16)$$

But the linearization of equation (9) is not obvious. Several hypothesis have to be checked:

- The assay sample and the reference sample have an identical matrix;

- All actinides have the same coefficient a_i on a limited energy range.

Then, on a limited energy range, equation (9) can be simplified and linearized:

$$ln(ln(\frac{1}{\Gamma(E)}) = ln(\sum_{i=1}^{N} W_i\mu_i\,(E)x) = a_i \cdot ln(\mathrm{E}) + ln\{\sum_i^N e^{b_i}\,W_i\,x\} \qquad (17)$$

In order to benefit from this linearized form, the data will be processed from the curve $ln(ln\left(\frac{1}{\Gamma(E)}\right) vs\, ln(\mathrm{E})$.

From xraylib library [5], we checked that actinides of interest, U and Pu, have the same values for the coefficient a_i on both sides of their respective absorption edge energy. The relative variations were found less than 0.5%.

In this work, all the values of $\Delta\mu_j(\mathrm{E}_j)$ were calculated from xraylib library.

4.1 Programming

The Python(x,y) [6] package was used to develop the spectrum processing software. The xraylib library software [5] was used to estimate the mass attenuation coefficients. Algebraic calculations and matrix data formatting are performed with the functions of the Python Numpy package.

The convolution algorithm was selected for smoothing the spectra [7]. This method is based on the convolution of a scaled window with the signal. The signal is prepared by introducing reflected copies of the signal (with the window size) at both ends so that transient parts are minimized at the beginning and end of the output signal. Window widths between 5 and 10 channels (for a typical spectrum on 2048 channels) are used. The hanning window was retained [7].

The user interface was created with PyQt. The Matplotlib [8] library is used to display the different plots.

4.2 Linear extrapolation to the discontinuity energy: "extrapolation algorithm"

This method is based on the use of equation (13). To calculate the concentration of actinide j, we have to determine the value of H_j that is the values of $A_{E_j^-}$ and $A_{E_j^+}$at the K-edge energy E_j. From the curve $ln(ln\left(\frac{1}{\Gamma(E)}\right) vs\, ln(\mathrm{E})$, and for each actinide, H_j can be estimated from extrapolations of the two linear regressions which were achieved on both side of absorption edge (cf. fig 2).

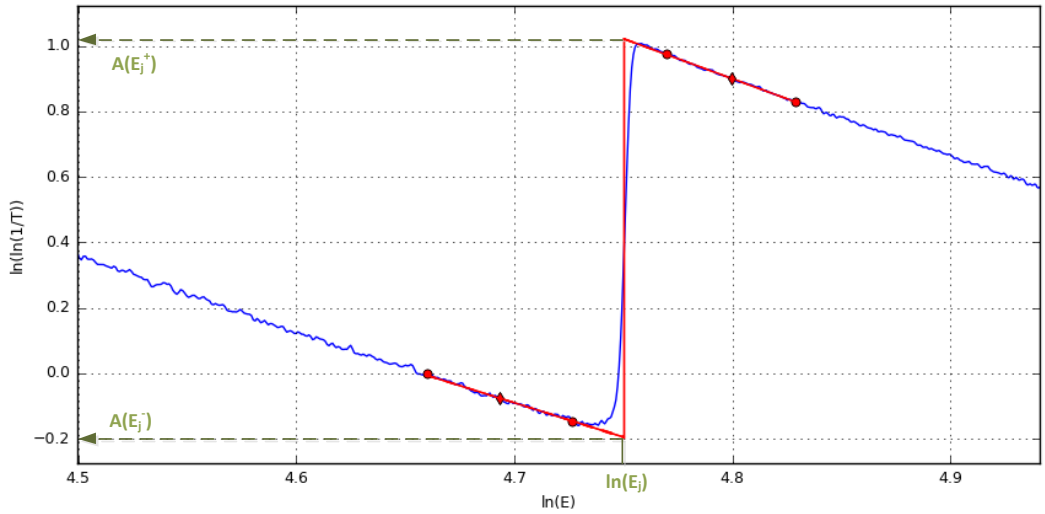

Figure 2. Example of method by extrapolation on Uranium K-edge discontinuity

4.3 Matrix algorithm

This algorithm is based on the use of matrix equation (14) or (15). It is the recommended algorithm by [1,3]. To calculate the concentration of actinide j, the values of $A_{E_j^-}$ and $A_{E_j^+}$ have to be estimated at two energies E_j^- and E_j^+ on both sides of absorption edge energy (cf. fig. 3).

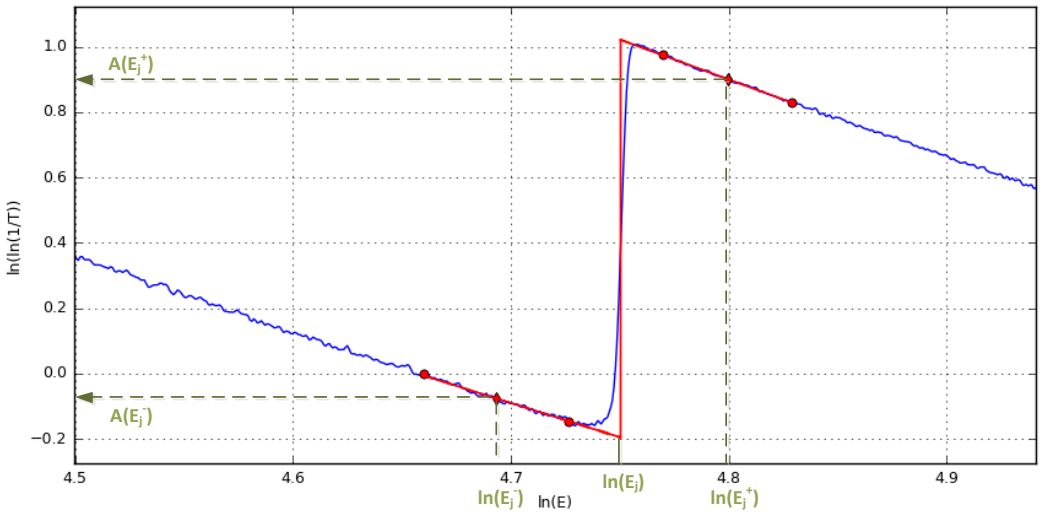

Figure 3. Example of "matrix method" on Uranium K-edge discontinuity

4.4 Checking and adjusting energy calibration of detector

^{109}Cd sources are used by several HKED systems, located on the side of HPGe detector, for energy calibration and to check gain stabilization. Our system having no sources, X-ray artefact peaks of lead (72.80 and 74.97 keV) and peak(s) on derivative KED spectrum attributable to absorption edge(s) (115.60 keV and/or 121.79 keV) are used to check and finely adjust calibration gain if needed.

4.5 Choice of energy ranges for calculation

The main difficulties to data processing of K-edge spectra is the choice of energy ranges. From these ranges, linear regressions are calculated and several values are estimated. These ranges are schematized on fig 4 and delimited by the points A to F.

The authors in [1,3] suggest fixed ranges on both sides of U and Pu energy discontinuities and the calibration is achieved with these parameters. In this work, with no calibration, another approach is adopted with flexible choice of energy ranges.

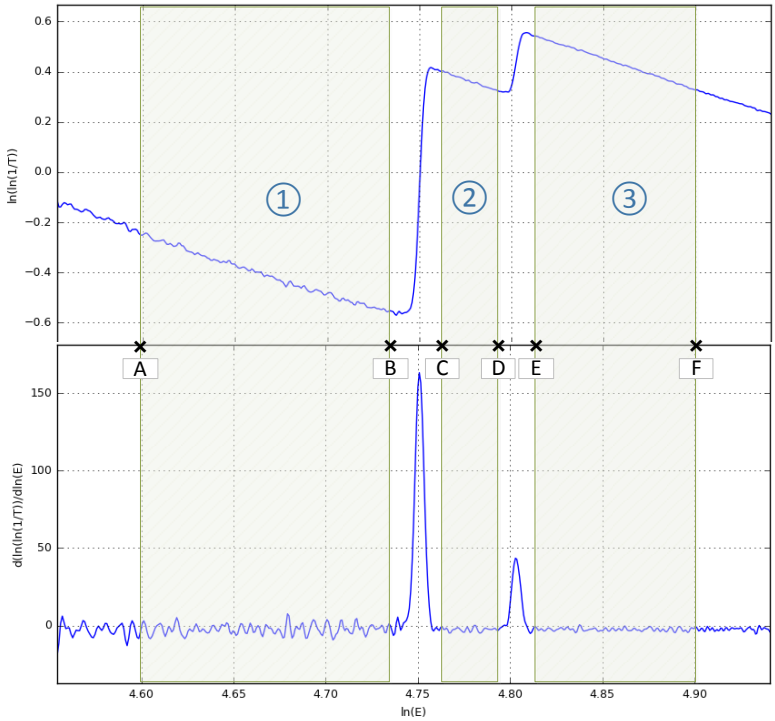

Figure 4. Definition of energy ranges used for data processing. Example with the absorption edges of U and Pu: three ranges are determined by the points A to F.

Moreover, taking advantage of computing power, calculations are achieved for each combination of points.

4.5.1 For extrapolation method

The principle consists in moving the points delimiting the linear regression area. For example the points A, B, C, D in case of Uranium concentration estimation. These points can take any position in their delimited area (zone 1 and 2). Linear regressions are achieved for each new position and uranium concentration estimated. Some restrictions are given for this computing: the minimum number of channel allowed for regression, the maximum number of channels being imposed by the width of area; the progression step.

Thus a histogram is plotted with the obtained results: each bar represent result frequency for the corresponding bin. The adjacent bins are taken of equal size. This size is determined from the mean of results by considering that the difference between two adjacent bin centers is less than x%. Lower is x, higher is the histogram resolution. The histogram maximum represent the most probable result. An example is given on Figure 6.

4.5.2 For matrix method

Unlike the previous algorithm, the linear regressions used in the matrix method have only a "smoothing" aim, and the fitted area is restricted to few channels (typically between 3 and 5). The selected values are the predicted y-values of these linear regressions for each center point x-values of delimiting area. Some restrictions are also given for this computing: the fixed number of channels allowed for regression, the maximum number of channel being imposed by the width of area; the progression step.

Thus a 1D or 2D-histogram is plotted according to the number of actinide (for this approach limited to 2). The resolution of histogram is determined in the same way as previously. For 2D-histogram, the most probable result is the couple of solution corresponding to the highest frequency. An example is given on Figure 7.

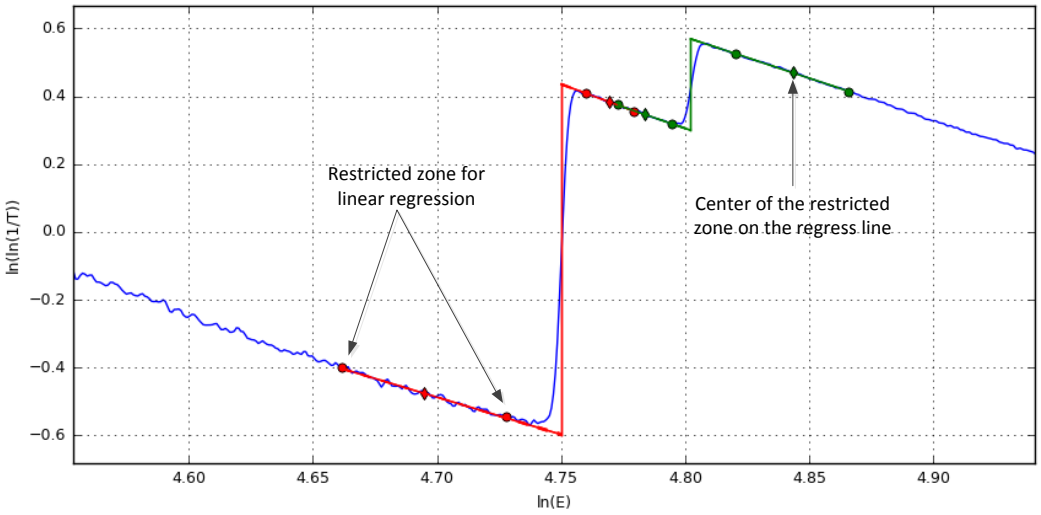

Figure 5. Definition of control points

5 Results

5.1 Method precision

For uranium measurement, in the 150 g/L-300 g/L concentration range for 3 trials of 1000 seconds live counting time, a counting precision of 0.22% has been documented [1].

As well, for plutonium measurement, in the 50 g/L-150 g/L concentration range for 3 trials of 1000 seconds live counting time, a counting precision of 0.23% to 0.18% has been documented [9].

Precision was studied with our device on uranium measurement. For each measurement, assay sample is send to counting station from hot cell to device (back shielded line) by pneumatic transfer. The precision estimation is based on the calculation of five concentrations by both algorithms. Thus, vial positioning and the method used for data processing are taken into account in the precision estimation. For uranium measurement, in the 150 g/L-300 g/L concentration range, a relative standard deviation of 0.25% for extrapolation algorithm and of 0.40% for matrix algorithm has been obtained using 1000 seconds as live counting time.

5.2 Comparison of the two approaches

First, Uranium EQRAIN standards supplied by CEA-CETAMA were used to study the influence of various parameters on the two algorithms (extrapolation vs. matrix).

Several reference spectra were recorded with different current intensities, from different preparations of reference solution (HNO_3 3 M), and for different dates. We noticed that the choice among these reference spectra can lead to substantial deviation in comparison with standard value (cf. Table 1 and Table 2). These deviations can be attributed to device stability (X-ray tube, current intensity, sample temperature). Extrapolation method seems more robust than matrix method (lower biases observed with the extrapolation method, see Tables 1 and 2).

The results obtained by the extrapolation algorithm are in very good agreement with the certified value (bias less than 0.3%).

In order to test if observed bias are significant, normalized deviation E_n was calculated according to:

$$E_n = \frac{C_{measured} - C_{reference}}{\sqrt{u_{reference}^2 + \left(\frac{s_{precision}}{\sqrt{n}}\right)^2}} \quad (18)$$

Where:

- $C_{reference}$ is the concentration of the certified reference material and $u_{reference}$ its standard uncertainty;

- $C_{measured}$ is the concentration estimated from algorithm and $s_{precision}$ is the corresponding precision standard deviation. Rigorously, global uncertainty should be considered. Here $s_{precision}$ doesn't take into account the other uncertainty contributions provided by X-ray tube stability, path length, reference solution (here HNO_3 solution only), background removal, etc.

- n is the number of measurements

If the value of E_n is not between -2 and 2 then the corresponding observed bias is considered as significant with an alpha risk of 5%.

For the extrapolation algorithm, all biases are non-significant but not for the matrix algorithm. This algorithm is more sensitive to variations on reference spectrum. It would be better to record reference spectrum in the same conditions on the same day as for assay sample. This observation suggests that the uncertainty chosen for the matrix algorithm, via $s_{precision}$, and for the E_n evaluation, is underestimated. By taking a standard uncertainty of 0.5%, the only bias identified is for reference solution R1 under 5mA.

Table 1. Estimation of uranium concentration by histogram approach with the extrapolation method (see text for more details). Minimum channels for linear regression = 25; step = 5; resolution = 0.1%.

EQRAIN U Certified value (g/L)	Estimated Concentration	Relative Deviation (%)	E_n	Reference solution and current intensity
361.77 ± 0.58 (k=2)	362.77	0.28	1.67	R1 5 mA
	362.57	0.22	1.34	R1 10 mA
	362.32	0.15	0.92	R3 5 mA
	362.09	0.09	0.54	R3 10 mA
	362.10	0.09	0.55	R4 5mA
255.20 ± 0.44 (k=2)	255.74	0.21	1.50	R1 5 mA
	255.17	-0.01	-0.08	R1 10 mA
	255.09	-0.04	-0.31	R3 5 mA
	255.11	-0.04	-0.25	R3 10 mA
	255.38	0.07	0.50	R4 5mA

Table 2. Estimation of uranium concentration by histogram approach with the matrix method (see text for more details). Number of channel for linear regression = 5; step=2; resolution=0.1%.

EQRAIN U Certified value (g/L)	Estimated Concentration	Relative Deviation (%)	E_n	Reference solution and current intensity
361.77 ± 0.58 (k=2)	358.85	-0.81	-3.33	R1 5 mA
	360.43	-0.37	-1.52	R1 10 mA
	361.91	0.04	0.16	R3 5 mA
	362.47	0.19	0.79	R3 10 mA
	361.60	-0.05	-0.19	R4 5mA
255.20 ± 0.44 (k=2)	253.26	-0.76	-3.85	R1 5 mA
	254.71	-0.19	-0.97	R1 10 mA
	256.26	0.42	2.08	R3 5 mA

	255.44	0.09	0.47	R3 10 mA
	255.09	-0.04	-0.22	R4 5mA

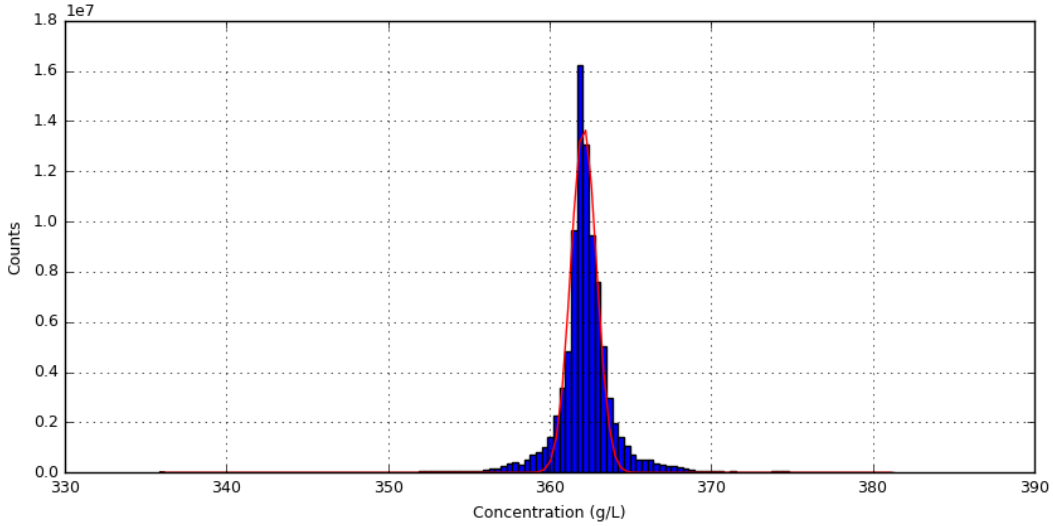

Figure 6. Histogram for Uranium (EQRAIN U) estimation from the extrapolation algorithm

In order to qualify these algorithms, several spectra supplied by IAEA acquired at the On Site Laboratory at the Rokkasho Reprocessing Plant were processed. These spectra were acquired from assay samples that contain high uranium and/or plutonium concentrations. Only path length and current intensities for assay sample and reference sample acquisitions are given. After processing, results were sent to IAEA and compared with IDMS results.

The two algorithms were used on these spectra and the results obtained are presented in Table 3 and Figure 8. The estimated values by the two algorithms are in good agreement with the IDMS values. For plutonium solution, estimations are less than 0.8% in comparison with IDMS values. None of the two algorithms is better. For mixed solution, uranium estimations are a little further to the IDMS values with an average relative deviation of 1% with the two algorithms.

The use of theoretical mass attenuation coefficient allow to obtain good results with low bias. The estimated uncertainties between 10 to 20% on mass attenuation coefficient proposed by [6, 7] seem too pessimistic near uranium and plutonium K edges. Indeed, according to equation (13), uncertainty on $\Delta\mu_j$ directly propagate on estimated concentration. Nevertheless, the positive bias observed for plutonium estimation by extrapolation algorithm (except for one case) would suggest that theoretical $\Delta\mu_{Pu}$ estimation need to be corrected. The best agreement between values obtained by extrapolation algorithm and IDMS values is reached with an increase of theoretical value of $\Delta\mu_{Pu}$ by only 0.33% that is 3.275 $g^{-1}.cm^2$.

Each result is the mean of three spectra. From results corresponding to five mixed (U, Pu) solutions measured three times, the mean precision standard deviation was calculated for both algorithms and for each element. Arbitrarily, these values have been chosen as standard uncertainties, for the matrix algorithm: s_U=0.44% and s_{Pu}=0.51%; and for the extrapolation algorithm: s_U=0.50% and s_{Pu}=0.74%. Considering these values, E_n has been calculated according to equation (18). For plutonium, the majority of the observed biases are non-significant while for uranium, nearly all the biases are significant.

In presence of high concentrated plutonium in solution, the bias on uranium concentration is higher than for single uranium solution. A bad estimation of background can be responsible

of such biases. Processing without taking into account the background subtraction has been studied. The results obtained are in Table 4.

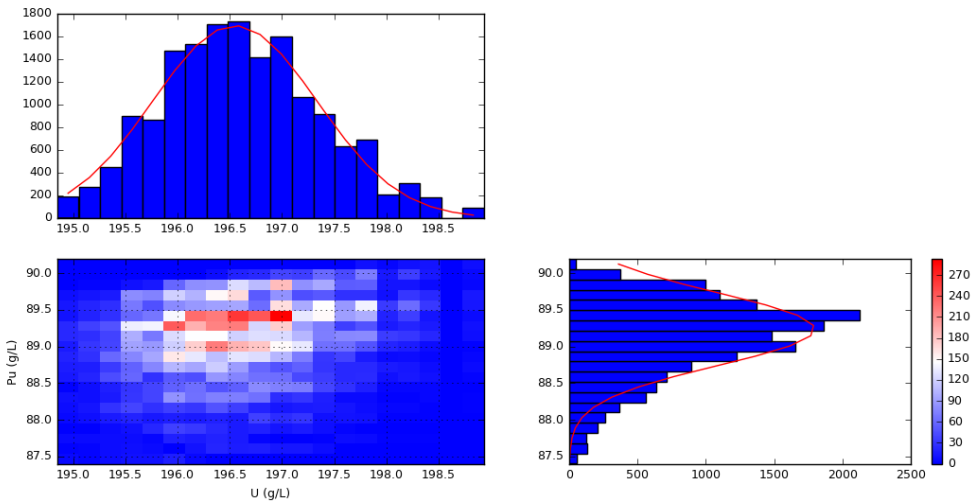

Figure 7. 2D-histogram for matrix algorithm processing on spectrum E.

Table 3. Estimation of U and Pu concentrations from spectra supplied by IAEA. Extrapolation parameters: 25 channels minimum for linear regression; step=5; resolution=0.1%. Matrix parameters: 5 channels for linear fit, step=2; resolution=0.1%. Reference spectrum, current intensity acquisition for assay sample and reference sample and path length were supplied by IAEA.

	IDMS – IAEA Results (±0.26% for K=2)		Extrapolation Algorithm		Matrix Algorithm		Relative deviation (%)				Extrapolation Algorithm		Matrix Algorithm	
Ref	U (g/L)	Pu (g/L)	U1 (g/L)	Pu1 (g/L)	U2 (g/L)	Pu2 (g/L)	ΔU1%	ΔPu1%	ΔU2%	ΔPu2%	$E_{n,U1}$	$E_{n,Pu1}$	$E_{n,U2}$	$E_{n,Pu2}$
3006	-	153.53	-	154.4	-	153.66	-	0.57	-	0.08		1.26		0.26
3101	-	150.11	-	150.69	-	149.62	-	0.39	-	-0.33		0.86		-1.02
3204	-	163.63	-	163.79	-	162.78	-	0.10	-	-0.52		0.22		-1.62
3205	-	86.40	-	86.22	-	85.99	-	-0.21	-	-0.47		-0.47		-1.48
3208	-	79.15	-	79.29	-	78.51	-	0.18	-	-0.81		0.40		-2.53
3268	-	156.61	-	157.74	-	156.59	-	0.72	-	-0.01		1.61		-0.04
3291	-	168.42	-	169.23	-	167.60	-	0.48	-	-0.49		1.07		-1.52
3315	-	78.29	-	78.62	-	77.95	-	0.42	-	-0.43		0.94		-1.35
2999	100.015	83.84	101.57	84.64	100.94	84.10	1.55	0.95	0.92	0.31	4.85	2.12	3.22	0.96
2888	197.134	90.87	198.97	90.83	199.02	90.32	0.93	-0.04	0.96	-0.61	2.92	-0.10	3.33	-1.89
2889	146.010	122.31	147.43	122.80	147.21	121.94	0.97	0.40	0.82	-0.30	3.05	0.89	2.86	-0.94
3215	205.03	94.28	206.75	94.91	206.17	93.03	0.84	0.67	0.56	-1.33	-2.63	1.49	-1.94	4.17
3217	205.49	94.26	206.62	95.18	206.78	94.18	0.55	0.98	0.63	-0.08	-1.73	2.17	-2.19	0.26
3230	114.95	96.51	115.67	96.32	115.78	95.51	0.63	-0.20	0.72	-1.04	-1.97	-0.44	-2.52	3.25
3283	118.46	99.43	118.89	99.67	119.71	98.90	0.36	0.24	1.06	-0.53	-1.14	0.54	-3.67	1.66
3309	127.20	106.85	127.35	107.30	129.30	106.83	0.12	0.42	1.65	-0.02	-0.37	0.94	-5.71	0.06

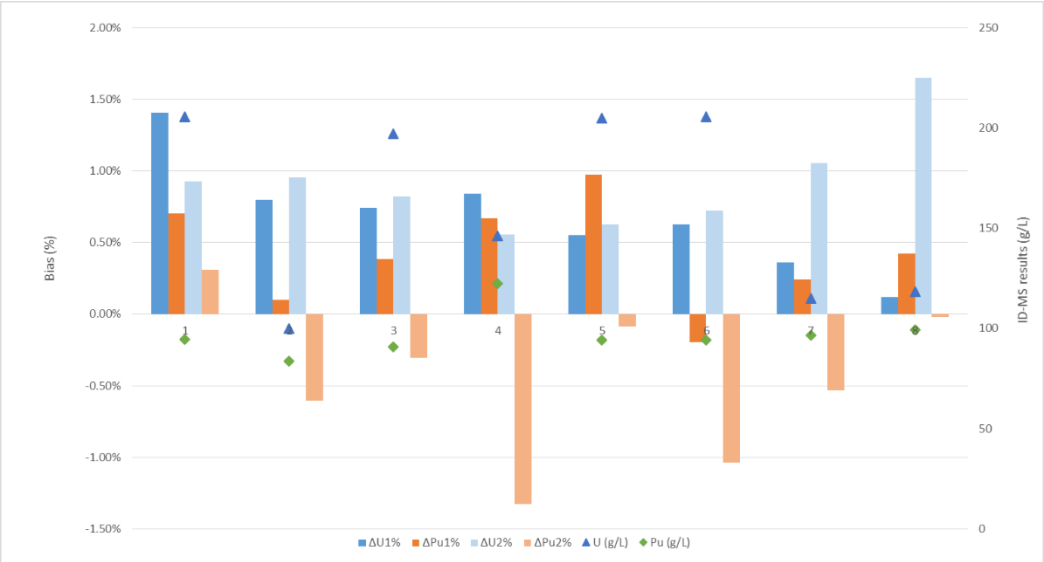

Figure 8. Bias on uranium and plutonium estimations by the two algorithms (see Table 3). Only results on mixed solution are represented.

Table 4. Estimation of U and Pu concentrations from spectra supplied by IAEA without background removal. Extrapolation parameters: 25 channels minimum for linear regression; step=5; resolution=0.1%. Matrix parameters: 5 channels for linear fit, step=2; resolution=0.1%. Reference spectrum, current intensity acquisition for assay sample and reference sample and path length were supplied by IAEA.

	IDMS – IAEA Results		Extrapolation Algorithm		Matrix Algorithm		Relative deviation (%)				Extrapolation Algorithm		Matrix Algorithm	
Ref	U (g/L)	Pu (g/L)	U1 (g/L)	Pu1 (g/L)	U2 (g/L)	Pu2 (g/L)	ΔU1%	ΔPu1%	ΔU2%	ΔPu2 %	$E_{n,U1}$	$E_{n,Pu1}$	$E_{n,U2}$	$E_{n,Pu2}$
3006	-	153.53	-	153.44	-	152.38	-	-0.06	-	-0.75		-0.13		-2.34
3101	-	150.11	-	149.61	-	148.94	-	-0.33	-	-0.78		-0.75		-2.44
3204	-	163.63	-	162.86	-	161.56	-	-0.47	-	-1.27		-1.06		-3.97
3205	-	86.4	-	85.73	-	84.86	-	-0.78	-	-1.78		-1.75		-5.62
3208	-	79.15	-	78.80	-	77.68	-	-0.44	-	-1.86		-0.99		-5.86
3268	-	156.61	-	156.83	-	155.24	-	0.14	-	-0.87		0.31		-2.74
3291	-	168.42	-	168.19	-	166.08	-	-0.14	-	-1.39		-0.31		-4.37
3315	-	78.29	-	78.15	-	77.15	-	-0.18	-	-1.46		-0.40		-4.58
2999	100.015	83.84	100.72	83.98	99.61	83.21	0.70	0.17	-0.40	-0.75	2.21	0.37	-1.42	-2.35
2888	197.134	90.87	197.14	90.04	196.99	89.43	0.00	-0.91	-0.07	-1.58	0.01	-2.06	-0.26	-4.99
2889	146.010	122.31	146.00	121.77	145.55	120.81	-0.01	-0.44	-0.32	-1.23	-0.02	-0.99	-1.11	-3.85
3215	205.03	94.28	204.02	93.81	203.56	92.26	-0.49	-0.50	-0.72	-2.14	-1.56	-1.12	-2.53	-6.78
3217	205.49	94.26	205.01	94.34	204.14	93.22	-0.23	0.08	-0.66	-1.10	-0.74	0.19	-2.31	-3.46
3230	114.95	96.51	114.55	95.55	115.01	94.62	-0.35	-0.99	0.05	-1.96	-1.10	-2.25	0.18	-6.19
3283	118.46	99.43	117.95	98.88	117.77	97.96	-0.43	-0.55	-0.58	-1.48	-1.36	-1.24	-2.05	-4.65
3309	127.2	106.85	126.32	106.48	127.39	104.95	-0.69	-0.35	0.15	-1.78	-2.20	-0.78	0.52	-5.61

Without background subtraction, plutonium results obtained with the matrix algorithm are degraded, while an opposite bias is observed with the extrapolation algorithm. Better results for uranium in mixed solution have been obtained by both algorithms. These observations outline how the background determination impacts the results. As previously, the E_n values have been calculated and if some biases on uranium concentrations have become non-significant, all biases on plutonium concentrations estimated by the matrix algorithm are significant now.

By proceeding spectra with the classical approach from the use of several single element calibration standard, Bosko *et al.* [10] underline observable biases on mixed solution results. They suggest the use of multi-elemental calibration standard in order to experimentally estimate all the terms of matrix in equation (14) and thus decrease the biases. Probably, this calibrating approach allows to compensate most of the systematic effects such as a bad approximation of background by adjusting the apparent mass attenuation coefficients.

The linearized plots have been compared with and without the background removal. For CEA assay sample with only high uranium concentration, the differences between the two plots are very small. For IAEA assay sample with high uranium and high plutonium concentrations, the observed deviation is on left side of the uranium discontinuity. This observation can't be generalized, the differences obtained with other CEA assay samples are non-significant.

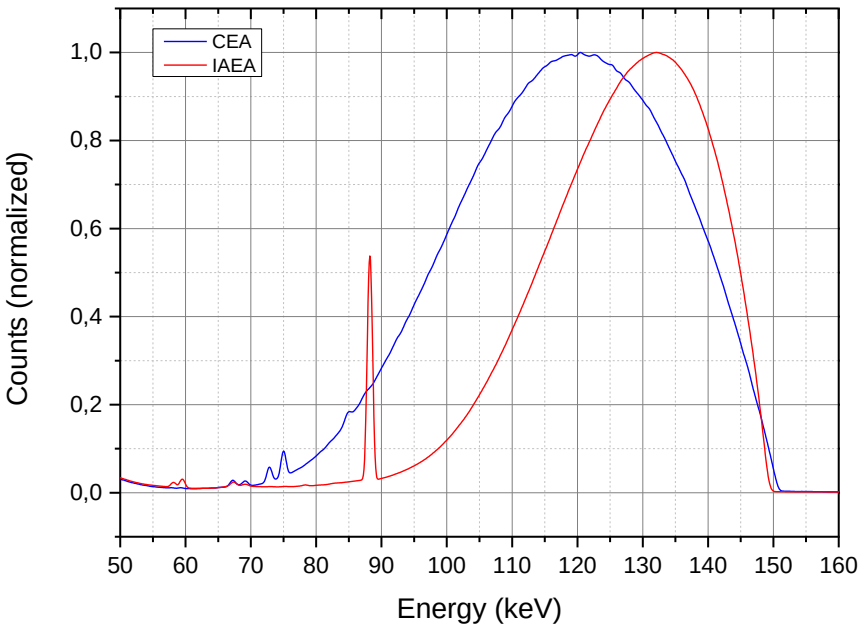

Figure 9. Comparison of reference spectra obtained by IAEA and CEA HKED devices.

The shapes of reference sample spectrum are plotted on Figure 9. These spectra have been normalized to make the comparison easier. The CEA spectrum is wider, primary beam is more scattered and/or less attenuated than IAEA one. Work on IAEA signal is more sensitive because a part of the spectrum (from 105 to 115 keV) presents a largest intensity variation for the same energy range than CEA signal. That explains the difference of sensitivity for background correction between CEA and IAEA spectra.

6 Conclusion

Two standardless algorithms were tested for K-edge spectra processing. Without calibration, it was not judicious to use fixed ranges for processing data, and nowadays, standard computer offers computation power that allows to easily study a lot of possibilities.

The first algorithm, called extrapolation algorithm, is more convenient for assay sample with only one high concentrated actinide because the choice of energy ranges for linear regressions is easier. Even with two high concentrations of actinides, the evaluations of concentrations of the two actinides by extrapolation method are almost independent (no covariance matrix term). The success of this method is linked to a good linearization of the different parts of the curve $ln(ln\left(\frac{1}{\Gamma(E)}\right) vs\, ln(\mathrm{E})$. As underlined previously, the use of a reference sample with the same matrix as assay sample is essential. But other sources can affect this linearization: accuracy of current intensity of X-ray tube, stability of electronic devices, and method used for background determination.

The second algorithm, called matrix algorithm, is less sensitive to linearization quality but more sensitive to variations on reference spectrum. The existence of a covariance term between U

and Pu plays an important role and, unlike the extrapolation algorithm, an inaccurate estimate for one involve an inaccurate estimate for the other.

Few data on the uncertainties of mass attenuation coefficients are available in the literature. Chantler [11] provides relative expanded uncertainties of several dozens of % near K-edges. Despite literature which does not recommend the use of estimated mass attenuation coefficients near edge energy, this study shows that some very good results are obtained with these values for uranium and plutonium concentration estimations, with a bias less than 1%.

The main parameters to take into account in order to improve these algorithms would be the background estimation by supposing no bias on the mass attenuation coefficient values.

In the laboratory, the two algorithms are implemented and their results are compared. The observation of a significant deviation indicates a problem in the measurement process (bad reference solution, or bad current intensity for example).

The detailed study of uncertainties for these two algorithms are in progress and will be the subject of a next paper. Even if there is no K-edge International Target Values (ITVs) for mixed U, Pu solutions, these uncertainties will be compared to the K-edge ITVs documented in [12] and based on solutions containing only high concentration of uranium or plutonium: 0.56% relative expanded uncertainties for uranium and 0.84% for plutonium.

7 Reference

[1] H. Ottmar, H. Eberle, The hybrid k-edge/K-XRF Densitometer: Principle – Design – Performance, Kernforschungszentrum Karlsruhe report Kfk 4590 (1991)

[2] Handbook of X-ray Spectrometry, 2nd ed., Revised and Expanded Edited by René E. Van Grieken (University of Antwerp) and Andrzej A. Markowicz (Vienna, Austria). Marcel Dekker, Inc: New York and Basel (2002)

[3] M. Collins, Generalized Multi-Edge Analysis for K-Edge Densitomertry, Proceedings of the 39th INMM Annual Meeting, Naples, FL (1998)

[5] T. Schoojans, A. Brunetti, B. Golosio, M. Sanchez del Rio, V. A. Solé, C. Ferrero, L. Vince, The xraylib library for X-ray-matter interactions. Recent developments, Spectrochimica Acta Part B (2011) 776-784

[4] R. D. McElroy, Jr., S. Croft, G. S. Mickum, S. L. Cleveland, Spectral Fitting Approach to the Hybrid K-Edge Densitometer: Preliminary Performance Results, INMM 56th (2015) Paper 518

[6] Python(x,y): a scientific-oriented Python distribution based on Qt and Spyder. Available from: https://python-xy.github.io/. Accessed December 2016

[8] Matplotlib. A Python 2D Plotting Library. Available from: http://matplotlib.org/. Accessed December 2016

[7] Scipy. Cookbook/SignalSmooth. Available from: http://scipy-cookbook.readthedocs.io/items/SignalSmooth.html. Accessed December 2016

[9] "Window based calibration of Hybrid K-Edge/XRF Spectrometer", H. Eberle, H. Ottmar, KFK report (Interner Bericht), December, 1993

[10] "Calibration of a Hybrid K-edge/XRF Densitometer (HKED) System for the Quantification of Mixed Uranium-Plutonium Solutions", A. Bosko, J-G. Decaillon, G. Duhamel, INMM 56th (2015)

[11] C.T. Chantler, "X-ray Form Factor, Attenuation, and Scattering Tables", J. Phys. Chem. Ref. Data 24 (1995) 71-643

[12] International Target values 2010 for Measurement Uncertainties in Safeguarding Nuclear Materials, IAEA STR-368, Vienna, November 2010